Geophys. J. Int. (1990) **102,** 551–562

Magnetic refraction studied on two experimental kilns

H. C. Soffel and K. Schurr*

Institut für Allgemeine und Angewande Geophysik, Universität München, Theresienstrasse 41, D-8000 München 2, FRG

Accepted 1990 March 12. Received 1990 March 12; in original form 1988 April 19

SUMMARY

Two experimental kilns in the form of shells (half-spheres) and circular bottom plates (inner radius: 15 cm, outer radius 17 cm) were made from clay, fire-clay and less than 5 per cent by volume of fine grained haematite powder for the study of the effect of magnetic refraction in archaeological structures. The haematite in the clay was reduced to a strongly magnetic phase (maghematized magnetite). The acquisition of TRM was performed in a non-magnetic gas-heated furnace in the local geomagnetic field. The kiln material has a maghemite ore content of about 2 per cent by volume and an apparent magnetic susceptibility at room temperature of about 4×10^{-2} SI units. The deviations of the declination and inclination of the TRM at different 'latitudes' of the shells were, respectively, up to 40° and 15° and systematically dependent from the position of the specimens in the shell or bottom plate in agreement with model calculations. However, the classical approach for the magnetic refraction in materials with ferrimagnetic ore grains dispersed in a non-magnetic rock matrix with simple assumptions for the demagnetizing fields of the ore grains and of the macroscopic sample was not able to explain the large refraction effects which have been observed. An adequate theory for the magnetic refraction in rocks is still not available.

For archaeomagnetic studies, some advice is offered for sampling and demagnetization treatment of the material in order to minimize refraction effects in archaeomagnetic data. Some consequences for palaeomagnetic studies are also discussed.

Key words: archaeomagnetism, magnetic refraction, palaeomagnetism.

1 INTRODUCTION

One of the most important and basic assumptions in palaeo- and archaeomagnetism is the parallel alignment of the thermoremanent magnetization (TRM) with regard to the external magnetic field. This assumption has been confirmed in the early years of palaeomagnetism by numerous measurements carried out on spherical or almost spherical rock samples like cubes or cylinders with equal dimensions of height and diameter. Here, the demagnetization factor is independent, of almost independent, of the direction within the specimen.

Since the early 1960s, some doubts about the perfect alignment of TRM parallel to an external field have been stated frequently, mainly in connection with studies on very accurately oriented (±0.5°) archaeomagnetic samples (Harold 1960; Weaver 1962; Aitken *et al.* 1964; Aitken & Hawley 1971; Thellier 1981; Clark, Tarling & Noël 1988). These doubts are not only based on studies of ceramics, tiles and bricks, but also on historical lava-flows (Tanguy 1970) in an area of known geomagnetic field direction. In some of the papers the scatter of magnetic directions was believed to be due to magnetic refraction effects, which are remarkable for instance in bodies like thin plates, hollow cylinders and spherical shells. Bodies like these are more often studied in archaeomagnetism than in palaeomagnetism.

The effect of magnetic refraction has also been studied by Strangway (1961), Vogt (1969) and Coe (1979). However, their theoretical approaches for the explanation of observed refraction effects remained unsatisfactory. Some authors (e.g. Dunlop & Zinn 1980; Aitken *et al.* 1986) have tried to estimate the likely refraction from the observed room temperature TRM and the estimated temperature dependence of the saturation magnetization. However, both effects are not strong enough to account for the observed distortion of the TRM directions.

During the investigation of medieval ovens from Herrenchiemsee in Southern Bavaria, having at least to

* Now at: Osram GmbH, D-7922 Herbrechtingen, FRG.

a certain extent the rather well preserved shape of half-spheres (Schurr 1983; Schurr, Becker & Soffel 1984), we found a systematic scatter of the horizontal component of the TRM direction within the structure. The effects could be explained qualitatively by assuming magnetic refraction, using the simple model of a long, hollow cylinder magnetized in a field perpendicular to the cylinder axis (see Fig. 6 in Schurr *et al.* 1984). Because of the poor conservation state of the ovens and the variable magnetic properties of the material it was not possible to carry out further systematic experiments with the intention of a quantitative interpretation. Therefore we decided to continue the study of magnetic refraction effects on bodies which fulfil the following requirements: (1) defined shape, (2) possibility for analytical model calculations, (3) well-defined direction and intensity of the geomagnetic field during TRM acquisition, (4) controlled temperatures during TRM acquisition, (5) known composition of the magnetic phases and well-defined grain sizes, (6) good mechanical consistency of the material, which should allow orientated core specimens to be taken with a precision of better than ±1°.

2 EXPERIMENTS WITH THE KILNS

2.1 Shape and composition of the kilns

The best shape to fulfil the above mentioned requirements was found be a half-spherical shell with a circular bottom plate. Ovens of a similar shape have been studied at Herrenchiemsee (Schurr *et al.* 1984). Two kilns have been made. The material for the experimental kilns consisted, respectively, of 63.6 (63.0) weight per cent clay (product 178/wf, see Schurr 1986) and 27.3 (30.0) weight per cent fire-clay, both without iron content, to which a certain amount of very fine grained haematite [9.1 (7.0) weight per cent, grain diameter: 0.8 μm, 97 per cent purity] was added. The shells and the bottom plates were made from the well-homogenized clay on a potter's wheel. After drying in air at 30°–35 °C for 2 weeks, they were fired in air in a normal electrically heated pottery oven at about 960 °C for about 10 hours to obtain a good mechanical consistency for the later experiments with TRM acquisition under controlled temperature, atmospheric and field conditions. The shells had an inner radius of 15 cm and an outer radius of 17 cm yielding a wall thickness of 2 cm. The bottom plates had also a thickness of 2 cm and a radius of 17 cm. After the first uncontrolled burning, the shells and bottom plates showed a reddish colour due to the haematite content.

2.2 TRM acquisition under controlled conditions

The production of an artificial TRM under controlled temperature and field conditions was combined with an experiment to reduce the weakly magnetic haematite in the ceramic shell and bottom plate into the more magnetic phases like magnetite and maghemite, which have been found as main carriers of remanence in the archaeological ovens at Herrenchiemsee.

A non-magnetic furnace was built at a site near the Geomagnetic Observatory Fürstenfeldbruck (FUR). It consisted of non-magnetic firebricks (see Fig. 1) with an inner diameter of about 50 cm, an outer diameter of about 120 cm and a height of about 60 cm. With a layer of firebricks, a completely horizontal plane was made for a well-defined position of the experimental kilns within the furnace. The top of the furnace was covered with layers of thin brick plates.

The direction and intensity of the local geomagnetic field was determined with flux gate magnetometers. The local values during the experiments (1985) were: $D \approx 0°$E, $I \approx 63°$, $T \approx 47\,400$ nT. They agree with the corresponding data at FUR. The direction of magnetic North was marked on the shells and the bottom plates for reference. The high temperatures were obtained with propane gas flames lead

Figure 1. Kiln within the opened non-magnetic furnace. White rod: a thermocouple leading into the centre of the kiln.

through openings of the furnace walls. The propane containers were kept at a safe distance from the furnace (≈10 m) for security reasons and to avoid a disturbance of the geomagnetic field at the place of the furnace.

The gas flames in the furnace provided a neutral or slightly reducing atmosphere outside the kilns. This was of course not sufficient for a reduction of the haematite in the shells and bottom plates into magnetite or maghemite. Therefore we filled the inner part of the kiln with well-dried sawdust, thus simulating the reducing conditions within the natural furnace material which are supposed to be due to the presence of organic matter (Le Borgne 1955).

The temperature outside and inside the kilns was measured at several places with non-magnetic thermocouples. It took about four hours to heat the kilns up to 750 °C, which is higher than the Curie temperature of haematite (675 °C). They were then cooled without additional measures in the closed furnace to the ambient temperature of about 20 °C within 20 hours.

2.3 Sampling of the kiln

From each of both shells, 96 drill cores (diameter: 2.5 cm; length; 2 cm) were taken normal to the surface of the shell using a specially made jig of wood for a proper positioning of the drill bit with regard to the shell (see fig. 3.2.1 in Schurr 1986). The position of each specimen has an accuracy of better than ±1° and can be described using two angles φ and λ, which are defined in Fig. 2(a). φ is the angle of latitude with reference to the bottom plate, while λ is the azimuth with reference to the magnetic north direction. The azimuthal difference between the specimens of constant latitude is 15°, thus 24 specimens could be drilled at the latitutes $\varphi = 5°$, 17°, 29° and 41°. The shell with drill holes is shown in Fig. 2(b). Specimens were not taken at higher latitudes than $\lambda = 41°$ because of the limited mechanical stability of the shells.

Specimens from the bottom plates (length: 2 cm; diameters: 2.5 and 1.25 cm, respectively) were drilled

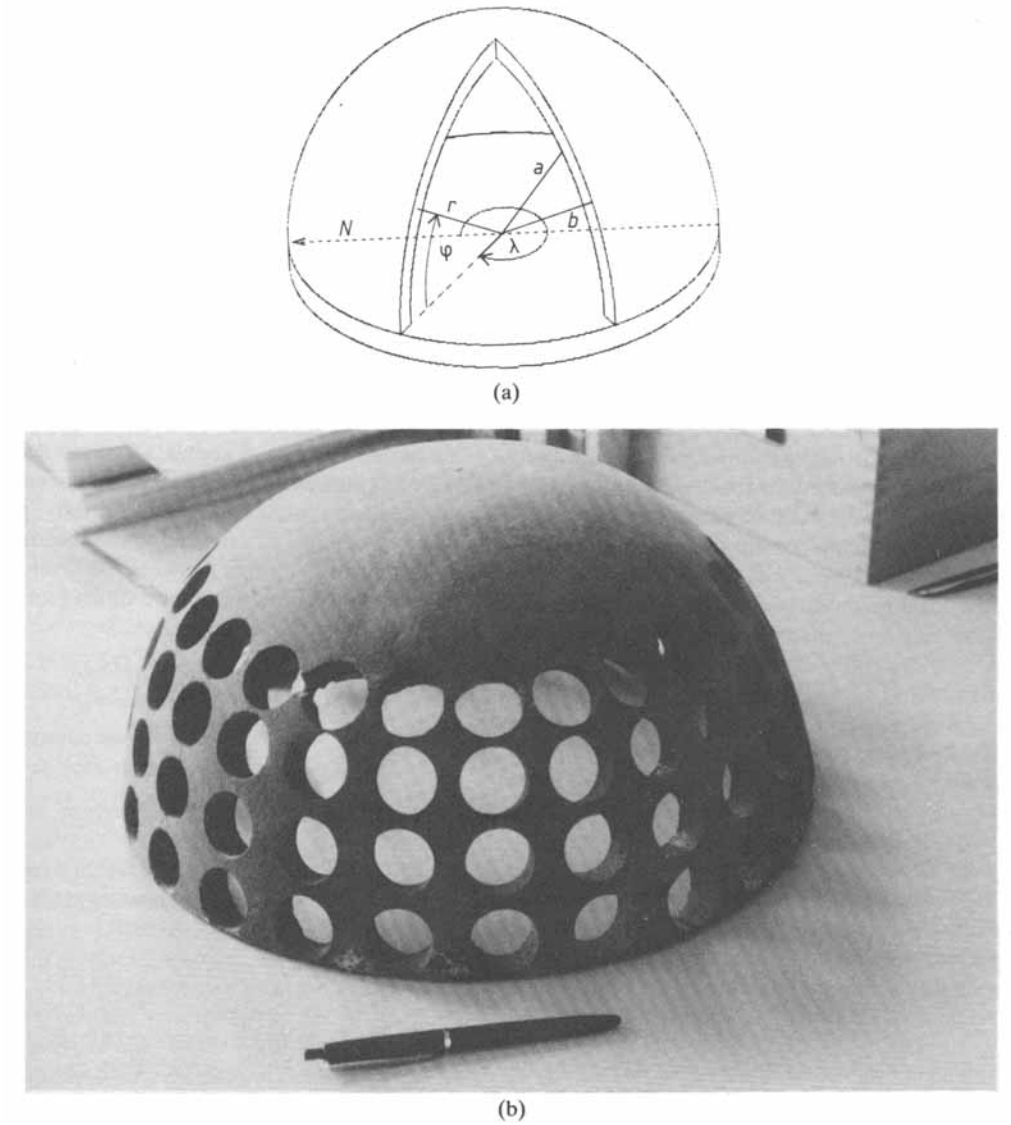

Figure 2. (a) Schematic sketch of the upper part of the kiln (half-sphere) with the definition of the parameters used for model calculations and sample positions. (b) Shell with drill holes.

normal to the surface. Their position on the plate can be described with the same azimuthal position angle λ as above and the distance r from the centre of the plate. A total of 162 and 69 cores were obtained from the bottom plates of kiln 1 and kiln 2, respectively.

A common feature of all specimens is a variation in colour from the inner to the outer part of the kiln. The inner part, pointing towards the centre, was black, the outer part was reddish and the central part was brown. While the black colour is due to remnants of the coal inside the kiln, the brown colour is indicative for magnetitie and/or maghemite and the reddish colour points to remnants of haematite.

2.4 Measurement of TRM directions

The remanent magnetization of the specimens was measured with a fluxgate spinner magnetometer. The magnetization intensities were quite uniform but different for both kilns due to the differences in the content of magnetic material. Histograms for the specimens of the shells from kiln 1 and kiln 2 are shown in Fig. 3. Mean intensity and directional data, specified for the shells, bottom plates and kilns are listed in Table 1 using conventional Fisher statistics. The declination data are referred to the horizontal component of the local geomagnetic field (with $D \approx 0°$ at the locality). The inclination is referred to the horizontal plane.

Table 1 shows that the mean TRM data are in part significantly different from the direction of the local geomagnetic field. The differences are not large compared to typical palaeomagnetic measurements, but they are severe with the regard to what is required in archaeomagnetism and for archaeomagnetic dating. However, the scatter is not random if one regards the TRM directions at a given latitude for different azimuth positions in the shells and at different azimuth positions in the bottom plates. As an example, Fig. 4 shows the declination values (a) and the inclinations values (b) of specimens from the shell of kiln 1 taken at a latitude of $\varphi = 29°$. Other examples for other latitudes of the shells and for the bottom plates of both kilns can be taken from Schurr (1986). The differences between the direction of the local geomagnetic field and the TRM of

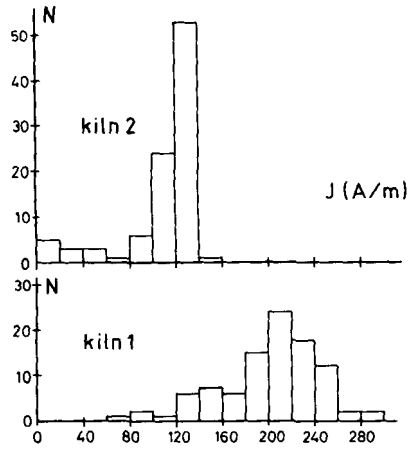

Figure 3. Histograms showing the intensity distribution of TRM of the shells of kiln 1 (a) and kiln 2 (b). For means and standard deviations see Table 1.

the specimens are up to 40° for the declination and up to 15° for the inclination (up to about 20° in 3-D space). The variation of the declination with the azimuth angle λ is roughly the same as in the ovens from Herrenchiemsee (Schurr *et al.* 1984). If means are taken for the entire bottom plate, for each latitude of the shells, for each shell or even for each kiln, the effects are averaged out; however, the precision parameters are still not very high and small α_{95} values can only be obtained from a very large number of samples, which is normally not available in an archaeomagnetic study.

Thermal demagnetization was carried out on various specimens in different longitude and latitude positions in order to find out whether the scatter of TRM is partly due to viscous components or components of different directions carried by magnetic material with different blocking temperatures. Fig. 5 shows a typical demagnetization plot (Fig. 5a) indicating that viscous remanence components with low blocking temperatures have only minor importance. The remanence is essentially monocomponent with main blocking temperatures between 500° and 550 °C (Fig. 5b). Beyond the Curie temperature of magnetite (580 °C) there is

Table 1. Mean declination $D(°)$ and inclination $I(°)$ of the shells, bottom plates and entire kilns and mean intensity data of TRM in A m^{-1} for the shells of both kilns. α_{95}: radius of the cone of confidence; k: precision parameter; N: number of specimens.

Subunit	D(°E)	I(°)	α_{95}	k	N	TRM
kiln 1						
bottom	4.4	+61.8	1.5	54.5	162	
shell	1.0	+63.6	1.9	61.3	96	20.0 ± 4.3
total	3.2	+62.6	1.2	56.3	258	
kiln 2						
bottom	356.6	+57.8	1.4	148.7	69	
shell	0.4	+66.5	1.4	100.9	96	11.0 ± 3.2
total	358.5	+62.9	1.2	87.3	165	
mean of all specimens from kiln 1 and kiln 2						
	1.4	+62.7	0.9	64.3	423	

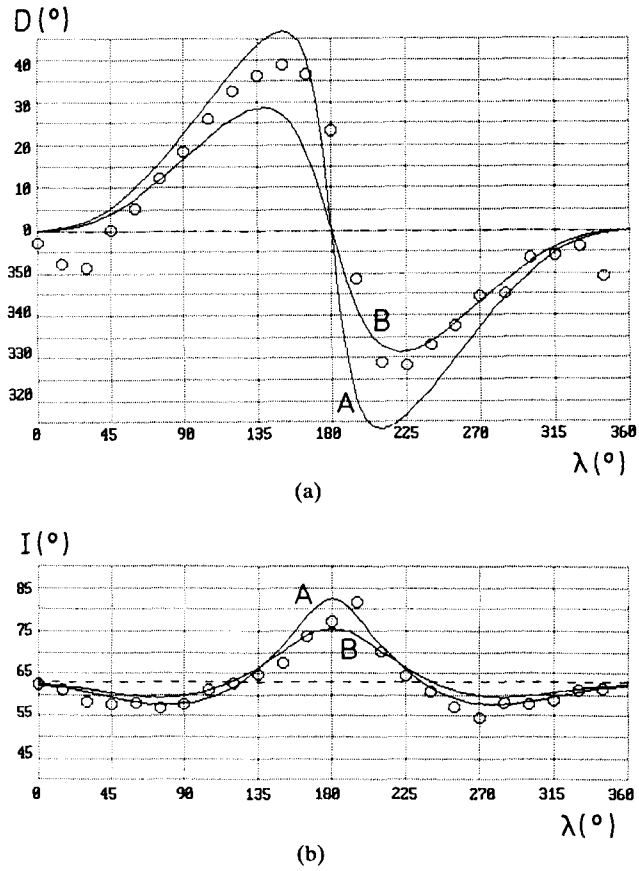

Figure 4. Variation of the declination D (a) and inclination I (b) with azimuth angle λ at a latitude $\varphi = 29°$. For definition of angles see Fig. 2. The curves A and B are model curves (see also Section 4 and Fig. 8) using a model susceptibility of 1 SI unit and $r = 15$ and 17 cm, respectively.

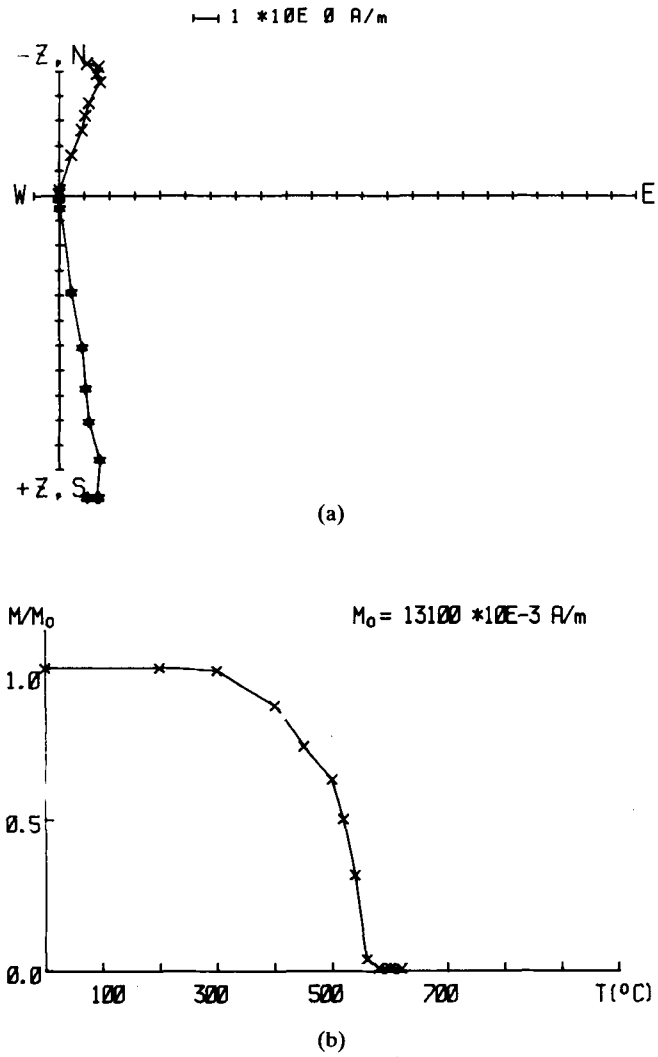

Figure 5. Variation of remanent magnetization during thermal demagnetization (a) of specimen number S2-20 from kiln 2. Crosses: projection into the horizontal plane; stars: projection into the vertical plane. The variation of the normalized remanence intensity is shown in Fig. 5(b).

still a significant remanence component left, with values for the declination and inclination, which are in a far better agreement with the direction of the local geomagnetic field ($D \approx 0°$, $I \approx 63°$) than those of the total TRM component. For details we refer to Table 2.

3 ROCK MAGNETIC PROPERTIES AND MAGNETIC MINERALOGY

3.1 Apparent magnetic susceptibility, its anisotropy and temperature dependence, coercive force

In text books on magnetism, the effect of magnetic refraction is dependent, besides geometrical parameters, mainly on the apparent magnetic susceptibility k_a of the material. This quantity was therefore measured at a frequency of 1000 Hz in a field of 302.5 A m^{-1} (3.8 Oe) with a Kappabridge KLY-2 (Geofyzika N. P. Brno, CSFR) at room temperature. As an example we give the values of the apparent reversible volume susceptibility (in SI units) at different latitude levels of the shell of kiln 1 in Table 3 to show also the variability of the parameter.

The anisotropy of the susceptibility k_a was also measured in order to see whether the process of making the shells and the bottom plates on the potter's wheel had any effect on the orientation of the magnetic minerals in the clay. Specimens from the shells and the bottom plates were measured in 15 different positions with the Kappabridge KLY-2. The anisotropy factor P, defined as the ratio of k_{max}/k_{min}, was in order of 1.05 with k_{min} in the direction normal to the surface of the shell or bottom plate, respectively. More details can be taken from Schurr (1986). It is sufficient to state here that the anisotropy of the magnetic susceptibility is small and of the order of 5 per cent or less. In any case it is too small to account for the large and systematic directional changes of TRM within the shells and bottom plates of both experimental kilns.

The temperature dependence of the apparent magnetic susceptibility was measured with a Highmoore susceptibility bridge at a frequency of 1000 Hz in a field of 800 A m^{-1} (10 Oe). This was made in order to test whether the Hopkinson peak, the susceptibility maximum at the blocking temperature immediately below the Curie temperature, can be made responsible for much larger susceptibility values than those observed at room temperature (see Table 3). Fig. 6 shows a plot of the magnetic susceptibility (normalized to

Table 2. Results of thermal demagnetization on specimens from the shell of kiln 2 taken at latitude $\varphi = 5°$ and different azimuth angles λ beyond 580 °C (Curie temperature of magnetite). Declination D, inclination I and TRM intensity data (in A m^{-1}) are given.

Specimen No.	Temperature	D(°E)	I(°)	(P)TRM?(A/m)
S2-1	NRM	5.5	77.7	11.854
	600°C	1.2	71.5	0.281
S2-2	NRM	347.9	78.2	11.768
	600°C	349.5	71.7	0.599
S2-3	NRM	340.6	73.2	11.768
	620°C	2.6	66.7	0.137
S2-4	NRM	333.1	66.8	12.649
	620°C	0.9	65.8	0.069
S2-5	NRM	340.1	68.8	13.489
	600°C	0.6	60.9	0.083
S2-6	NRM	342.8	65.9	13.089
	620°C	356.8	64.4	0.076
S2-7	NRM	358.5	66.0	13.165
	580°C	358.6	63.8	1.544
S2-8	NRM	5.4	63.6	13.496
	580°C	4.4	60.2	2.802
S2-9	NRM	8.9	65.5	13.993
	600°C	5.3	60.0	0.070
S2-10	NRM	11.9	65.9	13.143
	600°C	359.3	62.0	0.134
S2-11	NRM	12.5	68.5	12.251
	600°C	4.8	64.1	0.202
S2-12	NRM	6.8	70.6	11.582
	600°C	3.1	62.7	0.101

	D(°E)	I(°)	k	α_{95}(°)
Mean of TRM at 20°C:	356.6	69.8	133.8	3.5
Mean of PTRM at 580°-620°C:	0.9	64.5	354.6	2.2

Table 3. Apparent reversible volume susceptibility k_a (in 10^{-2} SI units) for different latitude levels of specimens from the shell of kiln 1. φ: latitude level, for definition see Fig. 2(a). MV: mean value; Min, Max: minimum and maximum values, respectively; N: number of specimens.

Level	Specimens No.	MV	Max	Min	N
$\varphi = 5°$	S1-1 - S1-24	4.023	6.288	2.245	24
$\varphi = 17°$	S1-25 - S1-48	3.920	5.262	2.317	24
$\varphi = 29°$	S1-49 - S1-72	3.899	4.825	2.458	24
$\varphi = 41°$	S1-72 - S1-96	4.482	5.688	3.176	24
All	S1-1 - S1-96	4.081	6.288	2.245	96

the value at room temperature) for two specimens from the shell of kiln 1. Both curves are reversible. Curve (a) stems from unseparated material of the black part of the inner wall of a shell, while curve (b) is from likewise unseparated material from the central brown part of the drill core (see also 2.3). The magnetic susceptibility is increased by a factor not more than 1.8 with regard to the value at room temperature. The sharp drop of the curves at around 550 °C points to magnetite and/or maghemite as main magnetic phases. This is also evident from the thermal demagnetization experiments (see Fig. 5b) and will be discussed later.

According to Dunlop (1974), the Hopkinson peak is dependent on the grain size. Assuming magnetite as the main magnetic phase, the factor of 1.8 points to grain sizes between 0.2 and 0.5 μm. The mean coercive force resulting from the magnetite (maghemite) grains of specimens from the shells and bottom plates is about 100 Oe (10 mT). The value is compatible with the coercive force of spherical stressfree magnetite particles either precipitated from solutions (Levi & Merrill 1978; Dunlop 1986) or grown hydrothermally (Heider, Dunlop & Sugiura 1987; Heider 1988) in the size range between 0.2 and 0.5 μm.

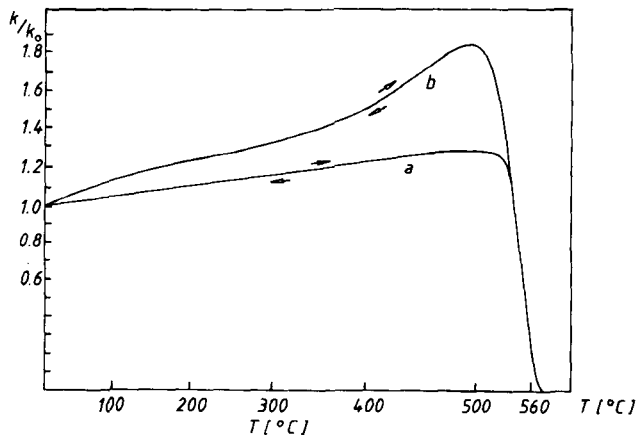

Figure 6. Normalized magnetic susceptibility k/k_0 as dependent on temperature. For details referring to curves (a) and (b), see text.

3.2 Temperature dependence of specific saturation magnetization

The variation of the saturation magnetization J_s with the temperature (J_s/T-curves) in heating and cooling cycles yields information about the Curie temperatures T_c and alteration of the magnetic phases during the heating experiments. Fig. 7 gives examples of the three types of normalized J_s/T-curves which have been obtained with a pendulum balance (Petersen 1961). Curves of the type shown in Fig. 7(a) were measured on unseparated and separated materials from the shells and the bottom plates. They indicate a single magnetic phase with a T_c slightly above 600 °C. The curves are completely reversible and show that the magnetic phase is resistent to oxidation at temperatures as high as 600 °C. Reversible J_s/T-curves of the type shown in Fig. 7(b) have some kinks indicating minor amounts of a magnetic phase with a T_c at around 160 °C and a second phase with a T_c near 560 °C. A more pronounced and irreversible curve is plotted in Fig. 7(c) also with two magnetic phases having T_c values of 160° and 560 °C, respectively. Curves of the latter types come from separated material from the outer and reddish part of the bottom plates. As will be shown in the next section, the phase with T_c around 160 °C is a titanomagnetite with x around 0.6 (TM60). However, irreversible J_s/T-curves and those with indications for a phase with T_c values around 160 °C were rarely observed. They occurred only in material from the outer reddish zones of the bottom plates. The bulk of the cores had reversible J_s/T-curves of the type shown in Fig. 7(a) with only one Curie temperature in the interval between 560° and 620 °C, which is indicative for magnetite and/or maghemite.

3.3 Optical and spectroscopic investigation of the magnetic minerals

The lattice parameters of the separated magnetic ore phase was analysed using the Debye–Scherrer method and Kobalt K_α rays. Material from the black inner, brown central and reddish outer zones of drill cores (see 2.3) from the shells and the bottom plates was investigated. The lattice constants of the magnetic phases and their abundance according to J_s

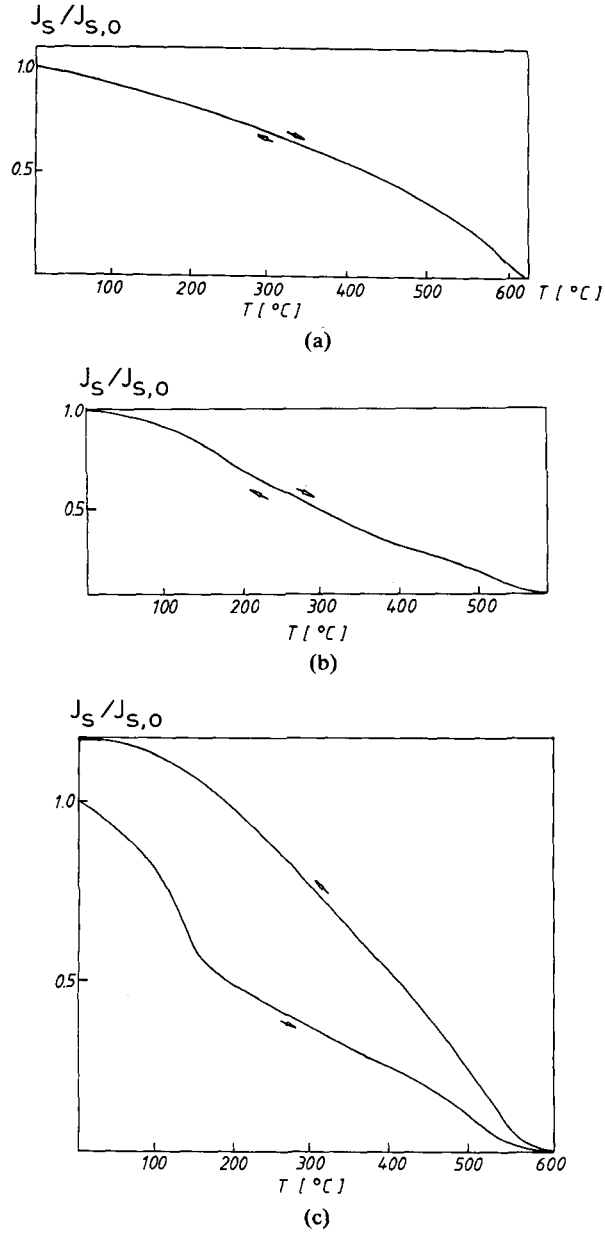

Figure 7. Temperature dependence of the normalized saturation magnetization $J_s/J_{s,0}$. (a) Reversible curve with only one Curie temperature at 620 °C. (b) Reversible curve with a Curie temperature at 560 °C and indications of a second phase with a Curie temperature at 160 °C. (c) Irreversible curve with two Curie temperatures at, respectively, 160° and 560 °C. For interpretation see text.

measurements on separated and unseparated samples are listed in Table 4. The ore content is of the order of 2 per cent by volume. In the inner black and in the central brown part of the drill cores (more than 80 per cent of each core) the dominant if not exclusive part of the magnetic ore fraction is maghemite. This is clearly identified by the lattice constant. Haematite is present only in traces in the outermost still reddish rim of the shells and bottom plates. Here, a TM60 can also be detected besides maghemite. The titanium comes from a Ti impurity in the haematite which was mixed into the clay (see 2.1).

Table 4. Identified magnetic phases, their lattice constants and abundance in the kiln material. S_i, S_c, S_o, B_i, B_o: inner, central and outer part of the shells and bottom plates, respectively. Lattice constant a_o is given in Å units (1 Å = 10^{-10} m).

Origin	magnetic phase	a_o (A)
S_i	maghemite (≈7.5% by weight, ≈3% by volume)	8.330 ± 0.002
S_c	maghemite (≈5% by weight, ≈2% by volume)	8.329 ± 0.002
S_o	maghemite and haematite	only faint lines
	(together ≈2.5% by weight, ≈1% by volume)	
B_i	magnetite and/or maghemite	8.381 ± 0.002
	(together ≈3% by weight, ≈1.5% by volume)	
B_o	titanomagnetite TM60,	8.474 ± 0.002
	maghemite and haematite	only faint lines
	(together ≈5% by weight, ≈2% by volume)	

In rocks, maghemite is in general a magnetic phase which is unstable with regard to heating experiments above 300°–400 °C decaying into the mineralogically more stable component haematite. It is surprising that maghemite in the kilns has such a high stability and the same Curie temperature as magnetite, although much higher T_c-values are reported for maghemite in the literature (675 °C). However, the presence of maghemite in burnt clays and soils is a common observation (Le Borgne 1955). The stability of the maghemite seems to be dependent upon the processes by which this phase is generated. Maghemite as a product of low-temperature oxidation, for instance during weathering, seems to be mineralogically less stable than maghemite produced at high temperatures from reduction of haematite and/or high-temperature oxidation of magnetite.

Mössbauer spectroscopy can also be used to distinguish between magnetite (with Fe^{2+} and Fe^{3+} ions) and maghemite with only Fe^{3+} ions. For details we refer to Schurr (1986). The presence of maghemite besides haematite (the ratio can be estimated as 70:30) as main carriers of remanence could be confirmed. However, the isomeric shift is not the same as for a pure maghemite phase. It would therefore be better to call the maghemite phase in the kiln material a maghematized magnetite. This would also explain its good mineralogical stability with regard to heating experiments.

Polished section studies showed the presence of very small (<1 μm) unclustered grains which could not be studied further by this method due to its limited magnification (<1200). However, scanning microscope studies were able to identify almost spherical ore grains with an average diameter of about 0.5 μm, which are most likely the main magnetic phase (maghemized magnetite). The optically observed mean diameter of 0.5 μm confirms the mean grain diameter derived from the observed Hopkinson peak and from the coercive force (see Section 3.1). The grains are presumably in the pseudo-single-domain stage with only few domains.

4 MODEL CALCULATIONS FOR THE FIELD DIRECTION WITHIN A SPHERICAL SHELL

Here only a very brief deduction of the formulae can be presented. For details we refer to Schurr (1986). Similar model calculations can also be taken from Rikitake (1987). The position of the points within the shell can be taken from Fig. 2. Besides the latitude φ and the azimuth λ, we define a as the inner and b as the outer radius of the shell and r as the distance of a point in the shell from its centre. It has not been attempted to compute the field direction within the model of our experiments (half-sphere on top of a circular bottom plate) rigorously. An analytical solution seemed to be impossible so far because of the complicate geometry of the model and the need to combine spherical functions (for the sphere) with cylindrical (Bessel) functions for the bottom plate. Therefore the model of an entire sphere was used as a first approximation for the field distribution within the half-sphere (closed by a bottom plate) at latitudes larger than, say, 10°–15°. Because of this approximation, our main conclusions with regard to magnetic refraction were drawn from data at a latitude of $\varphi \geq 25°$.

The shell may have a relative permeability μ_r. For the computation of the field lines within the shell walls we have to evaluate the magnetic field **H** and the magnetic induction **B** at each point at any angle and at distances $a \leq r \leq b$. We can deduce the magnetic field **H** from a scalar potential ϕ_M:

$$\begin{aligned} &\mathbf{H} = -\text{grad}\ \phi_M, \\ &\text{div}\ \mathbf{B} = 0, \\ &\mathbf{B} = \mu_r \mu_0 \mathbf{H}. \end{aligned} \tag{1}$$

The potential $\phi_M = \phi_M(r, \lambda, \varphi)$ must be a solution of the Laplace equation:

$$\Delta \phi_M = 0. \tag{2}$$

The general solution is given by the spherical function

$$\psi_n^m = (Ar^n + Br^{-(n+1)})[K \cos(m\lambda) + L \sin(m\lambda)]P_n^m, \tag{3}$$

P_n^m being the associated Legendre functions of degree n and order m. The following geometrical relationships are valid:

$$\begin{aligned} x &= r \cos\varphi \cos\lambda, \\ y &= r \cos\varphi \sin\lambda, \\ z &= -r \sin\varphi, \\ r &= (x^2 + y^2 + z^2)^{1/2}. \end{aligned} \tag{4}$$

For $D = 0°$ we obtain for $r > b$ the following expression for ϕ_M:

$$\begin{aligned} \phi_{M1} &= -H_0(x \cos I - z \sin I) \\ &= -H_0 r(\cos I \cos\varphi \cos\lambda - \sin I \sin\varphi), \end{aligned} \tag{5}$$

where H_0 is the intensity of the (inducing) geomagnetic field at the site of the experiments. The general equations for the potential in the three different spaces ($r > b$; $a \leq r \leq b$ and $r < a$) are

for $r > b$:

$$\phi_{M1} = (-H_0 r + \alpha r^{-2})(K \cos\lambda + L \sin\lambda) \cos\varphi, \quad (6a)$$

for $a \leq r \leq b$:

$$\phi_{M2} = (\beta r + \gamma r^{-2})(K \cos\lambda + L \sin\lambda) \cos\varphi, \quad (6b)$$

for $r < a$:

$$\phi_{M3} = \delta r (K \cos\lambda + L \sin\lambda) \cos\varphi. \quad (6c)$$

The continuity of the tangential components of the magnetic field and of the normal components of the magnetic induction at $r = a$ and $r = b$ leads to a system of four linearly independent equations for α, β, γ and δ. The solution is

$$\alpha = H_0[(2\mu_r + 1)(\mu_r - 1)(b^3 - a^3)/N], \quad (7a)$$

$$\beta = H_0[-3(2\mu_r + 1)/N], \quad (7b)$$

$$\gamma = H_0[-3a^3(\mu_r - 1)/N], \quad (7c)$$

$$\delta = H_0(-9\mu_r/N), \quad (7d)$$

with

$$N = (2\mu_r + 1)(\mu_r + 2) - 2a^3 b^{-3}(\mu_r - 1)^2. \quad (7e)$$

In order to calculate the unknown constants K and L, we can use the condition that the components of the magnetic field calculated from ϕ_{M1} must be identical with the components of the earth magnetic field for $r \gg b$. Finally we get as solution for the potential within the shell walls:

$$\phi_{M2} = (\beta + \gamma r^{-3})(x \cos I + z \sin I). \quad (8)$$

The three orthogonal components of the magnetic field within the shell walls (H_x, H_y and H_z) can now be calculated from $\mathbf{H} = -\text{grad}\ \phi_M$:

$$H_x = (x \cos I + z \sin I)3x\gamma r^{-5} - (\beta + \gamma r^{-3}) \cos I, \quad (9a)$$

$$H_y = (x \cos I + z \sin I)3y\gamma r^{-5}, \quad (9b)$$

$$H_z = (x \cos I + z \sin I)3z\gamma r^{-5} - (\beta + \gamma r^{-3}) \sin I. \quad (9c)$$

Now we are able to compute the declination D^* and the inclination I^* of the magnetic field within the wall of a spherical shell in dependence of the relative permeability μ_r and the position, described by r, φ and λ.

$$D^* = \arctan(H_y/H_x), \quad (10a)$$

$$I^* = \arctan[H_z/(H_x^2 + H_y^2)^{1/2}]. \quad (10b)$$

Model curves for the variation of the declination and inclination using a relative permeability of $\mu_r = 2$ (that means a susceptibility of 1 SI unit) and assuming an external inducing field with $D = 0°$ and $I = 63°$ are shown in Fig. 8 for the latitude values $\varphi = 0°$, 15°, 30° and 45°. The similarity between Fig. 8(c) ($\varphi = 30°$) and the measured variations of declination and inclination shown in Fig. 4 for $\varphi = 29°$ is evident, at least qualitatively. The main problem lies in the value for the magnetic susceptibility. The model calculations require a relative permeability $\mu_r = 2$, which means a susceptibility $k = 1$ SI unit following the relationship $\mu_r = 1 + k$, while the measurements of Section 3.2 yielded a mean apparent susceptibility at room temperature of only 4×10^{-2} SI units. The next section is therefore

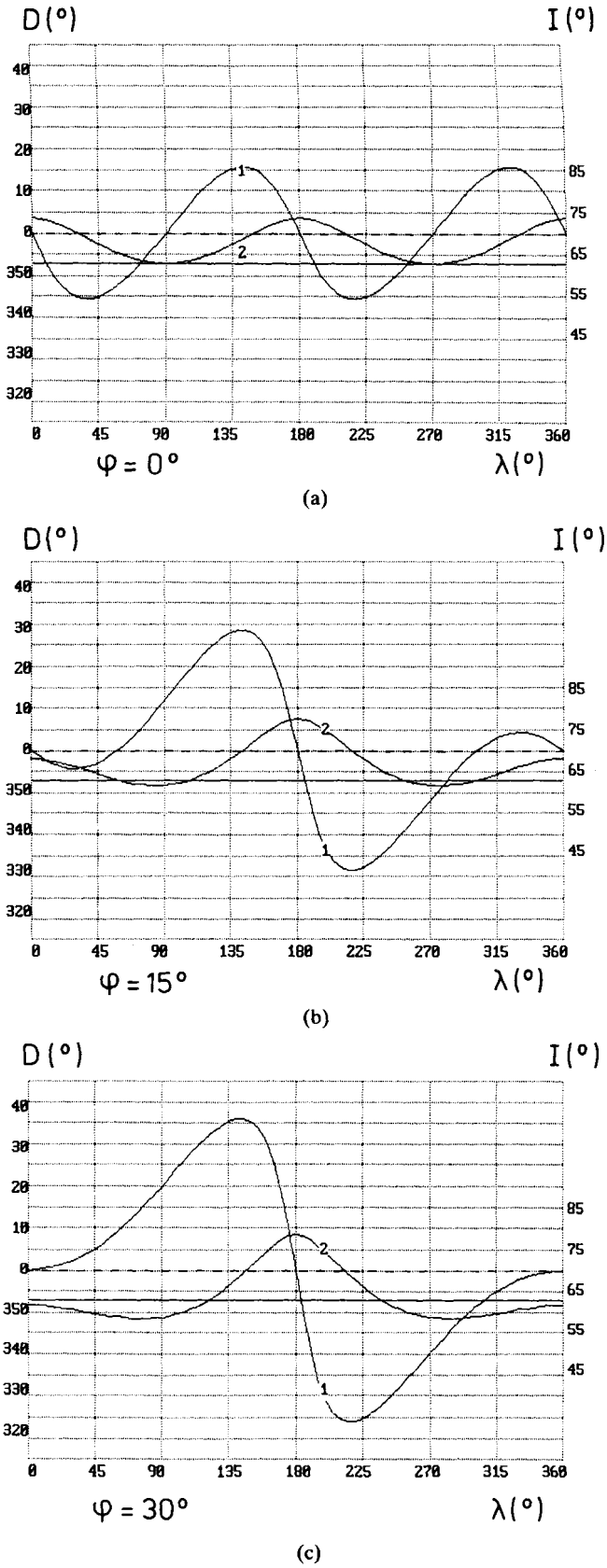

Figure 8. Model curves for the variation of declination D^* (curve 1) and inclination I^* (curve 2) within a shell as dependent on the azimuth λ at different latitudes φ. A model susceptibility k of 1 SI unit ($\mu_r = 1 + k = 2$) was used. (a) $\varphi = 0°$; (b) $\varphi = 15°$; (c) $\varphi = 30°$; (d) $\varphi = 45°$.

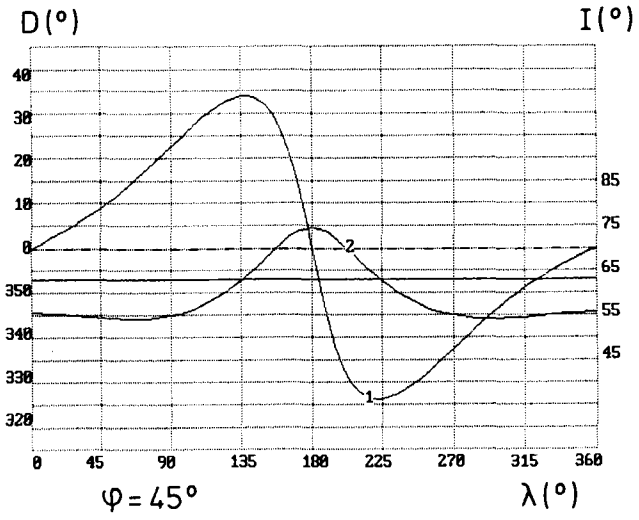

(d)

Figure 8. (*continued*)

devoted to a brief discussion of the classical theory of the magnetic refraction in materials containing equally distributed (not clustered) fine-grained spherical magnetic particles in a non-magnetic (mostly paramagnetic) matrix.

5 MAGNETIC REFRACTION

5.1 Simple theory

Magnetic refraction in bulk magnetic material is a well-treated subject in textbooks on magnetism and rock magnetism. With reference to Fig. 9, a magnetic field line may intersect a plane separating a vacuum with permeability μ_0 from a material with permeability μ_1, with $\mu_1 = \mu_0\mu_r$ and $\mu_r = 1 + k_i$ as the relative permeability and k_i as the intrinsic magnetic susceptibility.

The effective magnetic field H_{eff} is defined by the well-known relationship

$$H_{eff} = H_{ex} - NJ, \tag{11}$$

where H_{ex} is the external field, J is the magnetization and N is the demagnetizing factor. In our case of a plane interface (Fig. 9), the demagnetizing factor N_p parallel to the plane is 0, while N_n normal to the plane is 1. With $J = k_i H_{eff}$ we get

$$J = k_i H_{eff} = k_i(H_{ex} - NJ) = H_{ex}k_i/(1 + Nk_i) = H_{ex}k_a, \tag{12}$$

with $k_a = k_i/(1 + Nk_i)$ as the apparent susceptibility for bulk magnetic materials with the demagnetization factor N.

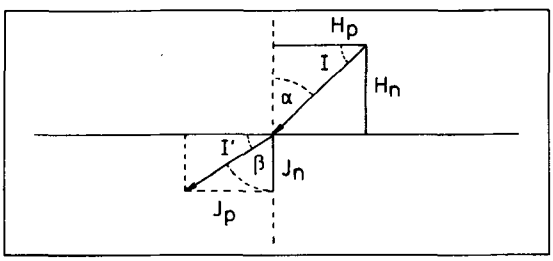

Figure 9. Magnetic refraction on a plane intersecting two materials with different permeabilities μ_0 and μ_1. See also text.

The external magnetic field H_{ex}, the apparent susceptibility k_a and the magnetization J can be separated into components parallel (index p) and normal (index n) to the plane. We get therefore using (12):

$$\tan\alpha = H_{ex,p}/H_{ex,n}, \qquad \tan\beta = J_p/J_n$$

and

$$J_p = H_{ex,p}k_{a,p} = H_{ex,p}k_i \tag{13}$$

due to $N_p = 0$ and

$$J_n = H_{ex,n}k_{a,n} = H_{ex,n}k_i/(1 + k_i)$$

due to $N_n = 1$.

From this we get the following relationship between the angles α and β:

$$\tan\beta = (1 + k_i)\tan\alpha = \mu_r \tan\alpha \tag{14}$$

as the law of magnetic refraction for bulk magnetic materials.

If we go from bulk magnetic materials to rocks, we have to consider a model containing in a first approximation highly diluted ferrimagnetic particles with a demagnetizing factor N_k in a non-magnetic matrix. The magnetization J_k of a single ferrimagnetic particle with an intrinsic susceptibility k_i is similar to (12) given by $J_k = k_i(H_{ex} - N_k J_k)$. Solving for J_k we obtain

$$J_k = H_{ex}k_i/(1 + N_k k_i) = H_{ex}k_{a,grain}$$

with

$$k_{a,grain} = k_i/(1 + N_k k_i). \tag{15}$$

The term $k_{a,grain} = k_i/(1 + N_k k_i)$ is also called the apparent susceptibility of the ore grain.

For rock samples, consisting of ferrimagnetic ore grains with the 'internal' demagnetization factor N_k, one has also to consider the 'external' demagnetization factor N_r of the macroscopic shape. Neglecting the contribution of paramagnetic minerals to the magnetization of the rock sample, its magnetization J_r can be described by $J_r = pJ_k$, with p as the volume fraction of the ore content. Equation (11) for the effective field can therefore be expanded (Angenheister & Soffel 1972) into

$$H_{eff} = H_{ex} - N_k J_k - N_r J_r = H_{ex} - N_k J_r/p - N_r J_r. \tag{16}$$

In analogy to (12) the magnetization J_r of the rock can then be expressed by

$$\begin{aligned} J_r &= pJ_k = pk_i H_{eff} = pk_i(H_{ex} - N_k J_r/p - N_r J_r) \\ &= H_{ex}pk_i/(1 + k_i N_k + pk_i N_r) = H_{ex}k_{a,rock}, \end{aligned} \tag{17}$$

when solving for J_r, where $k_{a,rock} = pk_i/(1 + k_i N_k + pk_i N_r)$ is the apparent susceptibility of the rock. In this case the law of magnetic refraction can be derived similarly to (13) as follows:

$$\tan\alpha = H_{ex,p}/H_{ex,n}, \qquad \tan\beta = J_{r,p}/J_{r,n}$$

$$J_{r,p} = H_{ex,p}k_{a,rock,p} = H_{ex,p}pk_i/(1 + k_i N_k)$$

due to $N_{r,p} = 0$ and

$$J_{r,n} = H_{ex,n}k_{a,rock,n} = H_{ex,n}pk_i/(1 + k_i N_k + pk_i)$$

due to $N_{r,n} = 1$ and hence

$$J_{r,p}/J_{r,n} = \tan\beta = [1 + pk_i/(1 + k_i N_k)]\tan\alpha. \tag{18}$$

Schurr (1986) proposed a law of magnetic refraction based on heuristic arguments [$\tan \beta = (1 + pk_i) \tan \alpha$], which is able to explain the observed refraction effect as well as the value of the apparent susceptibility. However, its physical basis is too weak and has therefore not been discussed in this paper in detail.

5.2 Comparison with the experimental data and conclusions

For the explanation of the actually observed magnetic refractions in the kiln shells a permeability of 2 or a susceptibility $pk_i/(1 + k_i N_k)$ of equation (18) of 1 SI unit is required from the model calculations. The observed value for the apparent susceptibility ($k_{a,rock} \approx 0.05$ SI units, measured on cylindrical specimens with a diameter to length ratio of 1.25:1) can be obtained from (17) by the reasonable value of $k_i \approx 15$ using $p = 0.02$, $N_k = 1/3$ as the 'internal' demagnetizing factor of spherical ore grains and $N_r = 0.2$ (Brown 1962) for the 'external' demagnetizing factor of the cylindrical specimens. Such high values for the intrinsic susceptibility k_i of maghemite seem to be plausible, because similar and even much higher values have been reported for magnetite (Kittel 1949; Smit & Wijn 1959). However, equation (18) limits μ_r to $(1 + p/N_k) = 1.06$ for large values of k_i. A value of $\mu_r = 2$, as required from the model experiments to explain the observed refraction effects, can only be obtained for $p = 0.02$ and $N_k = 1/3$ by the impossible assumption of k_i to be negative. This means that the hitherto proposed relations for the effective field H_{eff} (equation 16) and for the demagnetizing fields in rocks seem to be too crude and inadequate. Hashin & Shtrikman (1962) have proposed a theoretical model for the effective magnetic permeability of multiphase materials which includes as a possible solution the law of magnetic refraction proposed by Schurr (1986). However, their model requires a very special arrangement of magnetic and non-magnetic phases which is unlikely in rocks or burnt clays.

As mentioned earlier in this paper, experiments with TRM have almost exclusively been carried out so far on more or less spherical specimens (cubes, cylinders with $d/l \approx 1$), where magnetic refraction is not observed. We tentatively ascribe part of the scatter of TRM of thin lava flows to magnetic refraction effects and also refer to the paper by Tanguy (1970), who found magnetic refraction in a historical lava flow of Mount Etna in Italy. We think that it is premature to say that many palaeomagnetic data are affected by magnetic refraction effects. The study of Evans (1968) on thin vertical dikes from Western Australia showed that they seem to have recorded the ancient geomagnetic field correctly without refraction effects. However, we suggest to carry out TRM acquisition experiments on thin plates of rocks with dispersed fine-grained ferrimagnetic minerals of various concentrations and to develop a better theory of magnetic refraction for such materials.

Haematite with its much lower saturation magnetization compared with magnetite or maghemite, its much higher coercive force H_c and hence much lower intrinsic susceptibility [see Kittel (1949) for the relationship between H_c and k_i] should show little or no magnetic refraction effects. This can be confirmed (see Table 2), because the TRM carried by haematite with blocking temperatures above 600 °C is better aligned parallel to the external field than the TRM carried by maghemite and magnetite.

With regard to archaeomagnetic investigations, the scheme of sampling at as many different parts of the archaeological structures as possible, which has been proposed by Thellier, seems to be the most efficient method for the elimination of the refraction effects. As can be seen from Table 1, extremely large effects can be averaged out this way, but systematic deviations are still present and can become severe, when only parts of the archaeological structures are preserved for sampling. Thermal demagnetization beyond the blocking temperature of magnetite may help as well, because of much lower refraction effects in haematite. The refraction effects seem to be much lower in flat horizontal layers than in upright standing or dome-shaped structures. Furthermore there are places in all archaeological structures, where the refraction effects are insignificant and negligible (see Figs 4 and 8).

ACKNOWLEDGMENTS

We gratefully acknowledge the financial support by the Deutsche Forschungsgemeinschaft. Thanks are also due to the two referees (Professor Dr M. Aitken and Professor Dr M. E. Evans) and to the editor Professor Dr P. Weidelt for their very valuable comments and suggestions. We are also grateful for the discussion we had with Professor Dr K. Stierstadt and Professor Dr J. Schilling from the Physics Department of the University of Munich. Furthermore we appreciate the helpful discussions with Dr E. Appel, Dr S. Saradeth, Dr Ch. Bücker and Dr E. Schmidbauer.

REFERENCES

Aitken, M. J. & Hawley, H. N., 1971. Archaeomagnetism: Evidence for magnetic refraction in kiln structures, *Archeometry*, **13,** 83–85.

Aitken, M. J., Harold, M. R., Weaver, G. H. & Young, S. A., 1964. *A Big Sample Spinner Magnetometer and Demagnetizing Oven,* unpublished report, NATO Conference, Newcastle upon Tyne.

Aitken, M. J., Allsop, A. L., Bussell, G. D. & Winter, M., 1986. Palaeointensity determination using the Thellier technique: Reliability criteria, *J. Geomagn. Geoelectr.*, **38,** 1353–1363.

Angenheister, G. & Soffel, H. C., 1972. *Gesteinsmagnetismus und Paläomagnetismus. Studienhefte zur Physik des Erdkörpers 1,* Borntraeger, Stuttgart.

Brown, W. F., 1962. *Magnetostatic Principles in Ferromagnetism,* North Holland, Amsterdam.

Clark, A. J., Tarling, D. H. & Noël, M., 1988. Developments in archaeomagnetic dating in Britain, *J. archaeolog. Sci.*, **15,** 645–667.

Coe, R. S., 1979. The effect of shape anisotropy on TRM-direction, *Geophys. J. R. astr. Soc.*, **56,** 369–383.

Dunlop, D. J., 1974. Thermal enhancement of magnetic susceptibility, *J. Geophys.*, **40,** 439–451.

Dunlop, J. D., 1986. Hysteresis properties of magnetite and their dependence on particle size: a test of pseudo-single-domain remanence models, *J. geophys. Res.*, **91,** 9569–9584.

Dunlop, D. J. & Zinn, M., 1980. Archaeomagnetism of a 19th century pottery kiln near Jordan, Ontario, *Can. J. Earth Sci.*, **17,** 1275–1285.

Evans, M. E., 1968. Magnetization of dikes: A study of the palaeomagnetism of the Widgiemooltha Dike Suite, Western Australia, *J. geophys. Res.*, **73,** 3261–3270.

Harold, M. E., 1960. Magnetic Dating: kiln wall fall-out, *Archeometry*, **3,** 47–49.

Hashin, Z. & Shtrikman, S., 1962. A variational approach to the theory of the effective magnetic permeability of multiphase materials, *J. appl. Phys.*, **33,** 3125–3131.

Heider, F., 1988. Magnetic properties of hydrothermally grown magnetite crystals, *Thesis,* University of Toronto.

Heider, F., Dunlop, D. J. & Sugiura, N., 1987. Magnetic properties of hydrothermally recrystallized magnetite crystals, *Science,* **236,** 1287–1290.

Kittel, C., 1949. Physical Theory of Ferromagnetic Domains, *Rev. Mod. Phys.*, **21,** 541–583.

Le Borgne, E., 1955. Susceptibilité magnétique anormale du sol superficiel, *Ann. Geophys.*, **11,** 399–419.

Levi, S. & Merrill, R. T., 1978. Properties of single-domain, pseudo-single-domain and multi-domain magnetite, *J. geophys. Res.*, **83,** 309–323.

Petersen, N., 1961. Untersuchungen magnetischer Eigenschaften von Titanomagnetiten des Rauhen Kulm in Verbindung mit mikroskopischer und elektronenmikroskopischer Betrachtung, *MS thesis,* Universität München.

Rikitake, T., 1987. Magnetic and electromagnetic shielding, Reidel, Dordrecht.

Schurr, K., 1983. Archäomagnetische Untersuchungen an Feuerstellen aus Mannheim–Wallstadt und Öfen vom Herrenchiemsee, *MS thesis,* Universität München.

Schurr, K., 1986. Untersuchung des Einflusses der Formanisotropie eines magnetisierbaren Körpers auf die Richtung seiner thermoremanenten Magnetisierung, *Dissertation,* Universität München.

Schurr, K., Becker, H. & Soffel, H. C., 1984. Archaeomagnetic study of medieval fireplaces at Mannheim–Wallstadt and ovens from Herrenchiemsee (southern Germany) and the problem of magnetic refraction, *J. Geophys.*, **56,** 1–8.

Smit, J. & Wijn, H. P. J., 1959. *Ferrites,* Philips Technical Library, Eindhoven.

Strangway, D. W., 1961. Magnetic properties of diabase dykes, *J. geophys. Res.*, **66,** 3021–3032.

Tanguy, J. C., 1970. An archaeomagnetic study of Mount Etna: The magnetic direction recorded in lava flows subsequent to the twelfth century, *Archeometry,* **12,** 115–128.

Thellier, E., 1981. Sur la direction du champ magnétique terrestre, en France, durant les deux dernières millenaires, *Phys. Earth planet. Inter.*, **24,** 89–132.

Vogt, P. R., 1969. Can demagnetization explain seamount drift?, *Nature,* **224,** 574–576.

Weaver, G. H., 1962. Archaeomagnetic measurements on the Second Boston Experimental Kiln, *Archeometry,* **5,** 93–104.